Well-Defined Pillararene-Based Azobenzene Liquid Crystalline Photoresponsive Materials and Their Thin Films with Photomodulated Surfaces

Shi Pan, Mengfei Ni, Bin Mu, Qian Li, Xiao-Yu Hu, Chen Lin, Dongzhong Chen, and Leyong Wang**

Photoresponsive materials (PRMs) have long been a hot topic and photomodulated smart surface is very appealing. Particularly, liquid crystalline PRMs are able to amplify and stabilize photoinduced orientation thanks to their self-assembling and ordering characteristics. Herein, the first pillararene-based azobenzene liquid crystalline PRM with well-defined structure is presented, which can avoid the usually ill-defined composition drawback of polymer PRMs and prevent the severe H-aggregation from suppressing or even completely blocking photoresponse in simple azobenzene derivatives. The pillar[5]arene-based macrocyclic azobenzenes with variant length spacers show wide temperature range smectic liquid crystalline mesophases and excellent film-formation property. The tubular pillar[5]arene macrocyclic framework provides sufficient free volume for azobenzene moieties to achieve reversible photoisomerization and photoalignment; thus, their thin films demonstrate excellent light-triggered modulation of surface free energy, wettability, and even photoalignment-mediated orientation of an upper layer discotic liquid crystal columnar mesophase. Such pillararene-based azobenzene liquid crystals represent novel and promising PRMs with extensive fascinating applications.

1. Introduction

There has been widespread and persistent interest in the application of photochromism and photoresponsive characteristics for developing novel smart systems,[1–3] bioinspired materials,[4,5] or even stimuli-responsive photonic polymer coatings.[6] With the introduction of photochromic mesogenic units such as azobenzene, liquid crystalline (LC) systems are endowed with interesting photoresponsive characteristics including photoisomerization and photoalignment,[7–10] and such photochromic LC materials impart a promising platform for constructing photoresponsive smart surfaces as a result of the combination of long-range ordering, mobility, and response to light stimulation.[3]

Actually, the self-assembling capability and ordered characteristic of LC system are of particular importance for manipulating photoalignment due to their amplifying photoinduced orientation of photochromic moieties and stabilizing the oriented states.[7] Azobenzene chromophores are the most widely used photochromic mesogenic units to bring about reversible photoisomerization, light-induced alignment and even conduce to macroscopic motion.[7,8,11,12] Azobenzene mesogenic chromophores in their solid thin films can achieve photoalignment according to the polarized direction or light propagation direction upon irradiation with linear polarized light or nonpolarized light.[7,8] For linear polarized light, the azobenzene chromophores will take an orientation perpendicular to the polarization direction of the actinic light, while for oblique nonpolarized light, the axis of stretched *trans* azobenzene is apt to align in parallel with the light propagation direction to minimize light absorption.[7,8,13–16] However, the realization of *trans*/*cis* isomerization photochromic transformation requires sufficient free volume and the photoalignment of azobenzene chromophores demands even more free space for the involved motion of the whole chromophore moieties.[1,7] For simple low molar mass azobenzene molecules in the bulk state, the photo-responsiveness is usually remarkably weakened or even completely suppressed due to severe H-aggregation.[7] Various strategies have been employed for the establishment of photoresponsive feature. On the one hand, azobenzene containing polymer films were intensively investigated and revealed quite promising due to the free volume introduced by the

S. Pan, B. Mu, Q. Li, Prof. D. Z. Chen
Key Laboratory of High Performance Polymer Materials and Technology of Ministry of Education
Collaborative Innovation Center of Chemistry for Life Sciences
Department of Polymer Science and Engineering
School of Chemistry and Chemical Engineering
Nanjing University
Nanjing 210093, China
E-mail: cdz@nju.edu.cn

M. F. Ni, Dr. X.-Y. Hu, Dr. C. Lin, Prof. L. Y. Wang
Key Laboratory of Mesoscopic Chemistry of Ministry of Education
Center for Multimolecular Organic Chemistry
School of Chemistry and Chemical Engineering
Nanjing University
Nanjing 210093, China
E-mail: lywang@nju.edu.cn

DOI: 10.1002/adfm.201500942

polymer backbone and film self-healing capability to prevent the damage in subsequent isomerization cycles,[17–19] while as pointed by Meijer that there existed a major drawback for photoresponsive polymer systems of their usually ill-defined composition due to the intrinsic polydispersity of the synthetic polymers.[20] On the other hand, as photoresponsive material (PRM) of well-defined structure, side-chain azobenzene dendritic LC systems demonstrated significantly promoted photoresponsiveness by diluting the azobenzene content with long aliphatic chains to effectively reduce the formation propensity of H-aggregation.[20,21] Moreover, introducing a rigid or semirigid framework with a cavity to provide sufficient free volume seems to be a sound solution. In an early impressive work reported by Ichimura et al., calixarene-based macrocyclic amphiphiles with photochromic azobenzene units tethered asymmetrically on one side were immobilized on a substrate and showed remarkable photo-triggered surface contact angle change and then even demonstrated a light-driven directional movement of a liquid droplet.[1] Furthermore, regulating the orientation of calamitic mesogens by surface-assisted photoalignment has been widely studied and in some cases showing remarkable amplifying effect functioning as so-called "command surface," which has come into being an excited field as pioneered by Ichimura and co-workers.[7,22–25] Whereas reports for modulating discotic mesogens were quite limited and mainly aiming at low orderly discotic nematic phase (N_D).[16,26,27] Discotic liquid crystals (DLCs) have attracted great attention due to their capability of self-assembling into columnar mesophases possessing 1D conductivity. In contrast with the relatively easy and rapid alignment of N_D phase, the alignment of DLC columnar mesophases is a quite slow process and remains a huge challenge.[28]

Pillararenes are a new generation of macrocyclic host compounds after representative preceding star hosts such as crown ethers, cyclodextrins, calixarenes, and cucurbiturils, which are a class of macrocyclic oligomers constructed by connecting hydroquinone units via methylene bridges at *para*-positions, thus shape unique symmetrical tubular skeleton[29–31] in sharp contrast with the asymmetrical basket-like structure of calixarenes. Recently, pillararene-based multistimuli-responsive supramolecular self-assembled systems in solution have aroused broad attentions,[32–39] among which photoresponsive azobenzene chromophores were also adopted in some cases.[36–39] Nierengarten et al. pioneered the synthesis of pillararene-based macrocyclic LC compounds by attaching 10 or 12 cyanobiphenyl benzoate ester units onto pillar[5]arene or pillar[6]arene skeleton and investigated the macrocyclic effects on their mesomorphic behaviors.[40,41] In this work, we present the preparation of the first pillararene-based LC macrocyclic azobenzene PRMs, and demonstrate their photo-modulated thin film surface properties, together with the photoalignment induced orientation of the upper layer DLC columnar mesophases. The tubular framework is utilized here for providing the free volume of photoresponsiveness, in remarkable contrast with the widely reported supramolecular assemblies built by using the pillararene cavity-size-dependent host–guest interactions,[32–39] and may bring along a new class of well-defined PRMs with excellent film formation and surface modulation capabilities.

2. Results and Discussion

2.1. Synthesis and Rational Molecular Design

The rationally designed pillararene-based LC macrocyclic azobenzene PRMs, denoted as Pillar[5]-S(n)-Azo, with two representative samples of the spacer methylene number $n = 4$ and 10 for comparison (**Figure 1**a and Figure S20, Supporting Information), have been readily prepared according to the standard cyclization protocol[42–45] and referring to Nierengarten's procedure[40,41] to tether ten azobenzene mesogens onto both rims of pillar[5]arene framework through click reaction with some modifications. The azobenzene functionalization of pillar[5]arene macrocycle core was safely carried out in a reverse way of the literature method[40,41] by employing pillar[5]arene with ten alkyne groups and mono-azide terminated azobenzene mesogenic precursors (see Supporting Information for details) to avoid adopting the dangerous intermediate pillar[5]arene with ten azide groups of underlying hazardous azide-concentration as noticed by Nierengarten et al.,[40,41] such "click chemistry" route with multialkyne functionalized pillararene has also been reported for the preparation of various pillararene-based functional systems.[46] The reaction intermediates and products were fully characterized, as the disappearance of the absorption peak of alkyne groups at 3291 cm^{-1} in Fourier transform infrared (FTIR) spectra indicated the completeness of the click reaction (Figure S21, Supporting Information). Since no expected molecular ion peaks were observed in our attempts to measure the molecular weights of Pillar[5]-S(n)-Azo ($n = 4$, 10) by matrix-assisted laser desorption/ionization time-of-flight (MALDI-TOF) mass spectra, high performance liquid chromatography (HPLC) measurements were performed with a C18 reverse-phase column, which showed a strong single sharp peak for both product samples (see the Experimental Section and Figures S18 and S19, Supporting Information), indicating their high purity and monodispersity.[40,41] Thus obtained Pillar[5]-S10-Azo and Pillar[5]-S4-Azo are essentially azobenzene macrocyclic oligomers of stoichiometric molecular weights 6349 and 5507, respectively, with abundant flexible long aliphatic chains via ether linkage, which demonstrated excellent film-formation property. Robust transparent thin films of high optical quality can be readily obtained on various substrates such as those uniformly deposited on quartz discs via a routine spin-coating method (Figure S28, Supporting Information). In solution, Pillar[5]-S10-Azo showed an almost identical UV–vis spectrum to that of the corresponding azobenzene mesogenic precursor in both shape and peak values, while in solid films the π–π^* absorption peak of Pillar[5]-S10-Azo exhibited only a modest 19 nm hypsochromic shift compared with its corresponding absorption in solution, which is in sharp contrast with up to 60 nm blueshift of the azobenzene mesogenic precursor (Figure S23, Supporting Information). Such spectroscopic behaviors revealed their different condensed state structures, and manifested remarkably reduced aggregation among pillar[5]arene supported azobenzene chromophores and effective free volume afforded by the macrocyclic skeleton, which constituted the basis of the pronounced photoresponse capability in their solid thin films of pillararene-based macrocyclic azobenzenes such as Pillar[5]-S10-Azo, in striking contrast with the

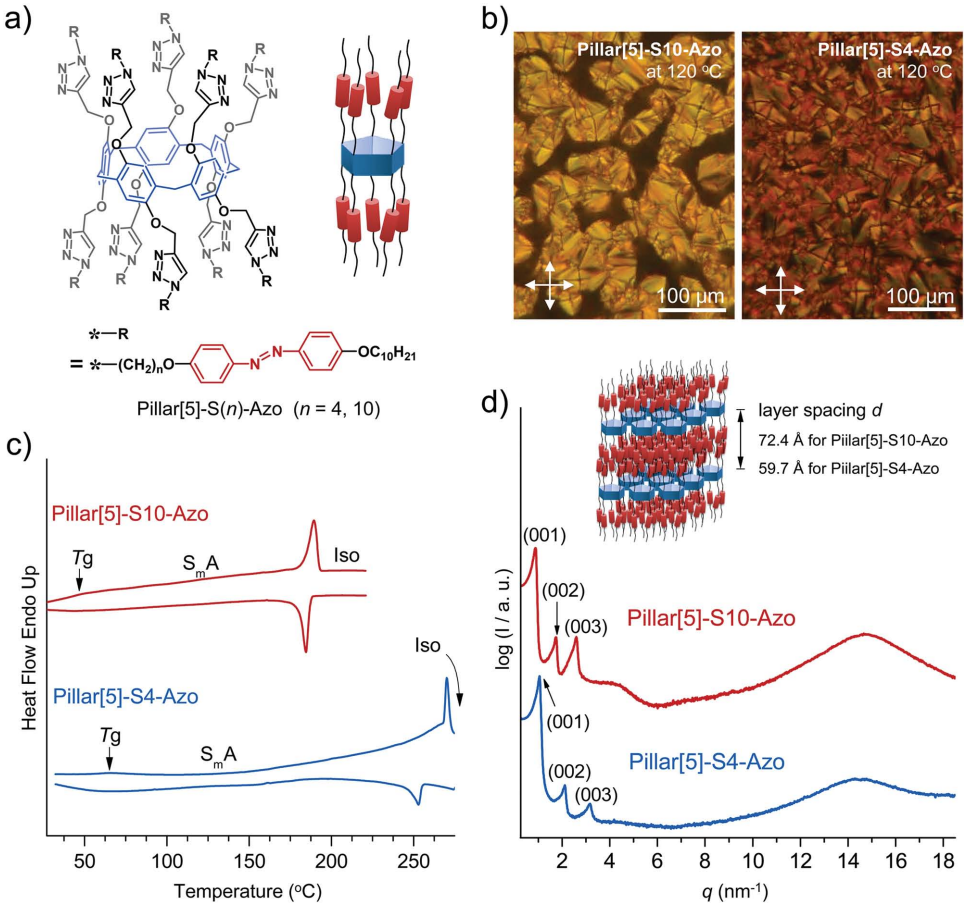

Figure 1. Chemical structure, thermotropic LC phase behaviors, and lamellar packing of pillararene-based macrocyclic azobenzene oligomers Pillar[5]-S(n)-Azo with spacer n = 4, 10. a) Chemical structures. b) Representative POM images within their LC range showing typical focal conic textures characteristic of S_mA mesophase. c) DSC thermograms showing smectic S_mA mesophases between glass transition and isotropization temperatures. d) SAXS/WAXS profiles at their LC state (80 °C) with the inset schematically illustrating the lamellar packing of S_mA phase.

complete photoresponsiveness suppression of their corresponding azobenzene precursors due to strong H-aggregation as in common low molar mass azobenzene derivatives.[7,21]

2.2. Thermotropic LC Phase Behaviors and Bulk State Packing Structures

Both Pillar[5]-S10-Azo (g 48.5 °C S_mA 189.4 °C Iso) and Pillar[5]-S4-Azo (g 63.2 °C S_mA 261.9 °C Iso) exhibited very wide temperature range smectic (S_mA) LC mesophases between the glass transition and clearing temperatures, as revealed by the typical focal conic textures under polarized optical microscopy (POM) observation (Figure 1b) and characteristic differential scanning calorimetry (DSC) thermograms (Figure 1c). Their lamellar periods were measured from small-/wide-angle X-ray scattering (SAXS/WAXS) analysis to be 72.4 and 59.7 Å, respectively, for Pillar[5]-S10-Azo and Pillar[5]-S4-Azo (Table S1, Supporting Information), with about 20% shorter than their estimated corresponding molecular contour lengths, suggesting a partially interdigitated packing structure (Figure 1d). Moreover, the lamellar structures were well retained with almost unchanged spacings upon lowering temperature to below the glass transition temperature as manifested by the temperature-dependent SAXS/WAXS analysis results (Figure S22, Supporting Information), which demonstrated that both pillararene-based macrocyclic azobenzene compounds possessed quite broad temperature range lamellar structure and exhibited frozen smectic mesophase at around room temperature, making up of the intrinsic basis for their serving as suitable LC PRMs. Furthermore, the significantly increased glass transition temperature 63.2 °C and isotropization temperature 261.9 °C of Pillar[5]-S4-Azo compared with 48.5 and 189.4 °C, respectively, for Pillar[5]-S10-Azo with longer flexible spacers, indicated that the pillararene-based macrocyclic azobenzene of shorter spacers assumed less flexibility and more compact packing.

2.3. Thin Film Photoisomerization Comparison of Pillararene-Based Macrocyclic Azobenzenes with Variant Length Spacers

Figure 2a,b shows the photo-induced isomerization evolution comparison of thin films of Pillar[5]-S10-Azo and Pillar[5]-S4-Azo under 365 nm UV irradiation, with thickness ≈350 nm spin-coated from 10 wt% tetrahydrofuran (THF) solution on quartz plates. The pristine films of pillararene-based

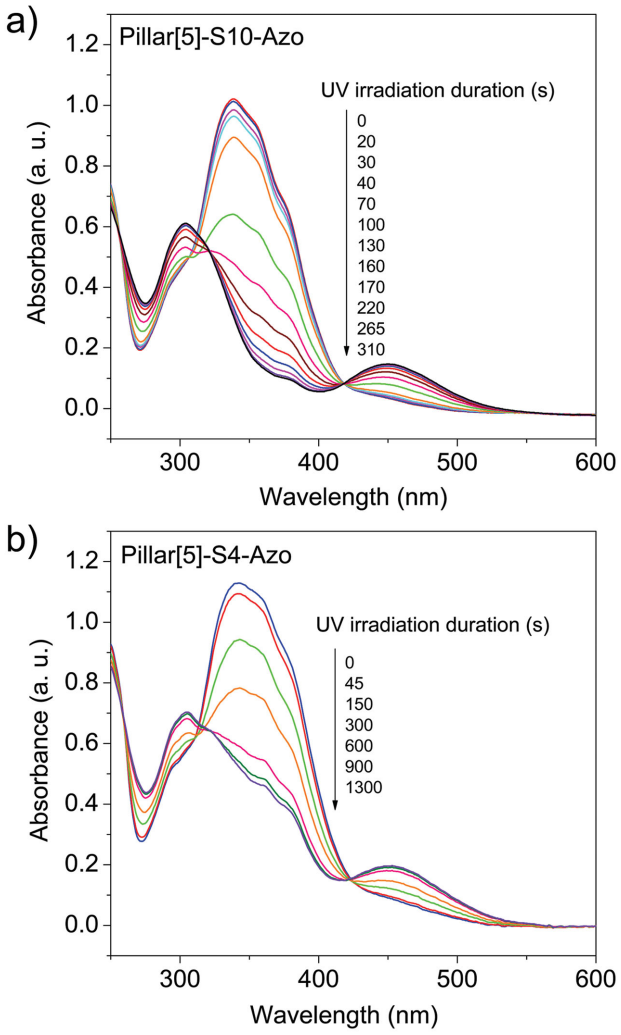

Figure 2. UV–vis absorption spectra evolution under 365 nm UV irradiation of thin films of a) Pillar[5]-S10-Azo and b) Pillar[5]-S4-Azo, the arrows indicating the intensity decreasing direction of the π–π^* transition peak around 340 nm with irradiation duration.

macrocyclic azobenzenes with variant length spacers displayed very similar UV–vis absorption spectra, and underwent *trans* to *cis* isomerization upon 365 nm UV irradiation with the characteristic π–π^* transition absorption peak of *trans* isomers at around 340 nm decreased, and two new peaks at about 300 and 450 nm of *cis* isomers emerged and gradually enhanced. The film of Pillar[5]-S10-Azo went through complete photoisomerization within about 5 min (Figure 2a), while in clear contrast, the *trans* to *cis* transformation of Pillar[5]-S4-Azo film of shorter spacers evolved slowly and could not reach completeness (Figure 2b). Even after prolonged UV irradiation for more than 20 min to guarantee reaching its photostationary state, a shoulder peak of π–π^* absorption still existed as shown in Figure 2b, which is even clearer from the direct comparison of their superimposed spectra (Figure S24, Supporting Information). With 450 nm visible light illumination, the absorption spectra of both films recovered through the back-isomerization process with the Pillar[5]-S4-Azo film recouped more rapidly due to its lower conversion extent (Figure S25, Supporting Information). Being a marked contrast to the different film performance, it was found that the absorption spectra of Pillar[5]-S10-Azo and Pillar[5]-S4-Azo in dilute solutions exhibited the same photoisomerization evolution tendency with perfect complete conversion and identical change rate upon UV irradiation (Figure S26, Supporting Information). Therefore, it indicated that there was no difference for pillararene-based macrocyclic azobenzenes with variant length spacers to undergo photoisomerization in dilute solutions in an unconstrained single-molecule state, while for the solid-state thin films, the free volume provided by the tubular pillar[5]arene architecture played a key role, manifesting that the molecular structure and intermolecular packing primarily determined their photoresponsive performance. Based on the above photoisomerization performance comparison, we chose Pillar[5]-S10-Azo with longer spacers to further examine their thin film photoresponse and surface properties.

2.4. Photoalignment of Pillararene-Based Macrocyclic Azobenzene Thin Films

2.4.1. 2D and 3D Alignment

Initially, 2D photoalignment has been readily demonstrated via 450 nm linear polarized light irradiation (Figure S29, Supporting Information). In the exposed stripe areas of the film shaped by a photomask, the directors of azobenzene chromophores of Pillar[5]-S10-Azo orientated perpendicularly to the polarized direction of the incident light and displayed bright stripes under POM observation in sharp contrast with the dark areas covered by the photomask during photoalignment, indicating appreciable degree of uniaxial orientation.[47,48] Moreover, 3D alignments were also well achieved via a long-time irradiation of nonpolarized actinic light (**Figure 3**). First, the spin-coated Pillar[5]-S10-Azo thin film of ≈350 nm in thickness was exposed to vertically incident nonpolarized 450 nm light for 1 h to induce the homeotropic orientation of azobenzene chromophores, and then followed by exposure to the same actinic light for 1.5 h through a photomask at an oblique angle of 45° to the film surface normal. Consequently, the azobenzene chromophores took a slantwise alignment in the obliquely irradiated stripes, showing bright field when the projection of oblique irradiation direction on the film plane deviated from the polarizers under POM observation (Figure 3b,d), while those areas covered by the photomask during the oblique light irradiation preserved the original homeotropic alignment and displayed dark field. When the irradiation direction projection coincided with one of the polarizers upon rotating the directions of crossed polarizers, the POM image turned totally dark irrespective of the orientation of azobenzene chromophores (Figure 3c).

2.4.2. Readily Achievable On–Off Switching of Photoalignment

The patterns created by photoaligned Pillar[5]-S10-Azo thin films can be well preserved up to 150 °C and kept almost

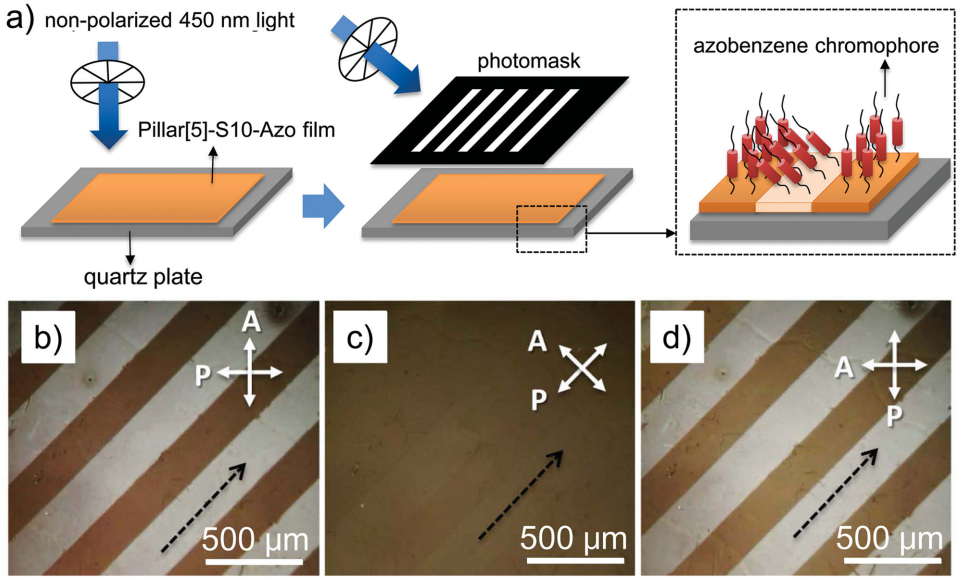

Figure 3. a) The schematic experimental set-up and cartoon showing mesogenic azobenzene chromophore orientations. b–d) POM images of the stripe patterned Pillar[5]-S10-Azo thin films on a quartz substrate with the film orientation at 45, 90, and 135° relative to the direction of the analyzer after a sequential irradiation of nonpolarized 450 nm light vertically and then obliquely through a photomask. The black dashed arrows indicate the projection direction of the oblique incident light on the film plane, and the white crossed arrows denote the directions of polarizer (P) and analyzer (A).

unchanged after at least 6 months showing satisfactory thermal stability and long-term retainability. Moreover, establishment, erasure, and recovery of such alignment can be readily realized by sequential light irradiation of variant wavelength or together with an annealing process, which may offer a new pathway for smart material design and surface property modification. For instance, the homeotropic alignment of azobenzene chromophores can be attained by either long-time vertical exposure to nonpolarized actinic visible light or through an annealing process,[13,49–51] and the *trans* to *cis* photoisomerization was reached by a short time irradiation of UV light followed by back-isomerization via a quick exposure to visible light; thus, a switchable on–off cycling of such homeotropic alignment was established as monitored by changes of UV–vis absorption spectra shown in **Figure 4**a,b. The as-coated pristine films displayed the strongest π–π^* absorption as dashed curves in Figure 4a,b, indicating their totally random alignment. After long-time exposure to vertical nonpolarized actinic visible light (Figure 4a) or a sufficient annealing process (Figure 4b), both π–π^* and n–π^* absorption intensities of the thin films remarkably decreased (green curves in Figure 4a,b), indicating azobenzene moieties took homeotropic orientation against the substrate plane. Then, subsequent UV irradiation resulted in typical absorption spectra of *cis* isomers (magenta curves in Figure 4a,b), indicating *trans* to *cis* photoisomerization, which consequently destroyed the homeotropic alignment due to the formation of bent-core *cis* azobenzene configuration. By subsequent quick visible light irradiation, *trans* configuration of azobenene chromophores restored with random orientation, showing the almost recovered strongest absorption peak (blue curves in Figure 4a,b). Starting from this point, once again by long-time exposure to vertical nonpolarized actinic light or annealing, the homeotropic alignment will be re-established and such cycling can continue in sequence as schematically shown in Figure 4c. It is worth noting that there exists a small difference in absorption intensity between the film recovered upon photoisomerization by UV irradiation (blue curves) and the pristine film (dashed curves), implying some orientation historical imprint in the recovered film in contrast with the totally random pristine film obtained from spin-coating. Whereas from the second cycle all succeeding on-off switching cycles exhibited excellent reversibility (Figure S27, Supporting Information).

2.5. Photo-Regulated Interfacial Properties

2.5.1. Oil Contact Angle

The outstanding photo-induced isomerization and orientation performance of Pillar[5]-S10-Azo thin film offer promising optical means to manipulate the solid surface properties. Considering the remarkable hydrophobic properties of the pillararene-based macrocyclic azobenzene thin films, oil droplet contact angle measurements were adopted to well reflect the surface properties such as surface energy changes. As shown in the left column of **Figure 5**, a droplet of pure olive oil (5 μL) was dripped onto a pristine Pillar[5]-S10-Azo thin film of thickness ≈100 nm coated on quartz substrate. Upon irradiation with 365 nm UV light for gradually increased time up to 5 min, the contact angle gradually reduced from 31.1° of the pristine film to 12.4° accompanied with bit by bit spreading of the oil droplet, which indicated increase of surface free energy by generation of *cis* isomers with relatively higher dipole moment.[1] Furthermore, as shown in the right column of Figure 5, a long-time (1 h) vertical exposure to nonpolarized 450 nm actinic light first triggered the rapid *cis* to *trans* recovery process and then further induced the homeotropic alignment. With another

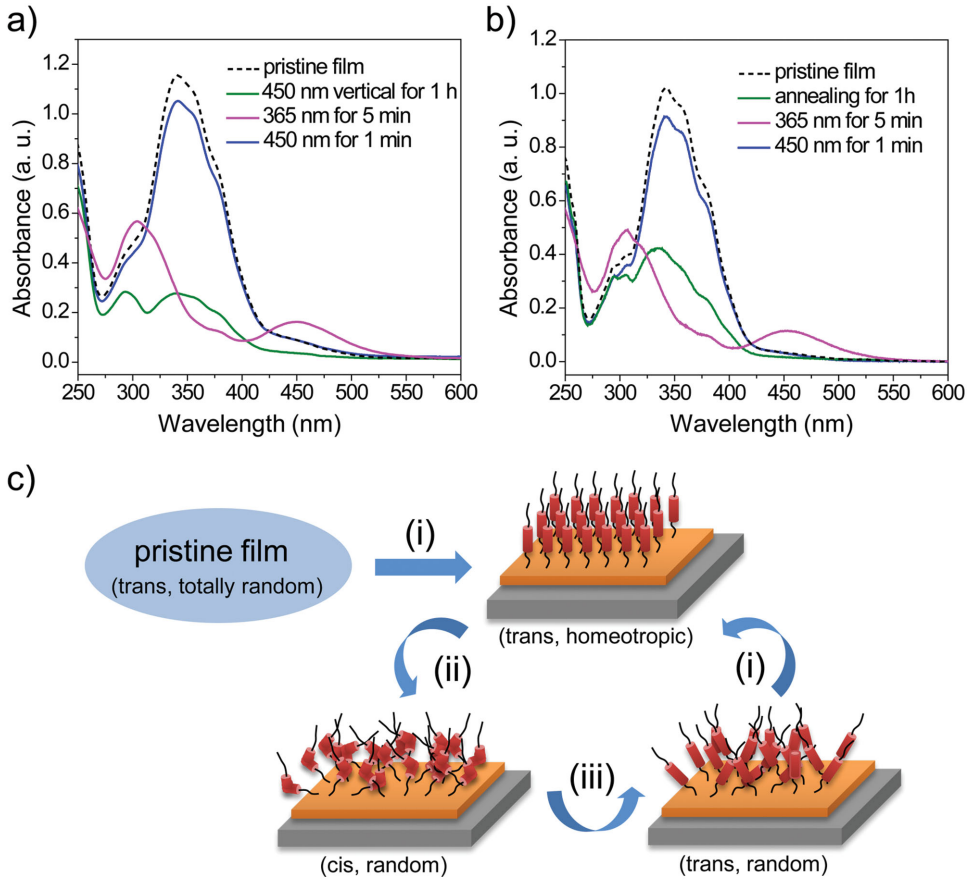

Figure 4. On–off switching of photoalignment. a,b) UV–vis absorption spectra changes of Pillar[5]-S10-Azo thin films on quartz plates showing on–off switching of homeotropic photoalignment induced by a) long-time vertical exposure to nonpolarized actinic 450 nm visible light or b) through an annealing process. c) Schematic illustration of the switchable on–off cycling of photoalignment in Pillar[5]-S10-Azo thin film upon (i) vertical exposure to 450 nm nonpolarized actinic light for 1 h or annealing at 100 °C for 1 h; (ii) 365 nm UV irradiation for 5 min; (iii) 450 nm visible light irradiation for 1 min.

5 µL olive oil droplet transferred onto this homeotropically aligned film of Pillar[5]-S10-Azo, the oil droplet displayed significant dewetting compared with the pristine film with contact angle increasing from 31.1 to 41.4°, which manifested that the vertical orientation of Pillar[5]-S10-Azo molecules with the aliphatic tails vertically protruding to the surface significantly reduced the surface free energy. It is interesting to note that the resulting smallest contact angle of 19.0° after reaching its photostationary state with UV light irradiation for 300 s was a little larger than that without photo-induced alignment (12.4°), indicating some memorial influence of the homeotropically aligned structure.

2.5.2. Photoaligned Surface-Mediated Migration and Orientation of DLC Columnar Mesophases

Aforementioned obvious spreading and dewetting phenomena of oil droplets on Pillar[5]-S10-Azo thin films indicated significant surface energy changes triggered by underlying azobenzene alignment, which was reminiscent of that both azimuthal and polar angles of azobenzene polymer thin films could be manipulated, as further applied to induce surface-assisted DLC N_D mesophase photoalignment through oblique irradiation of nonpolarized actinic light, as reported by Ichimura and co-workers.[16,26,27] Thus, we were encouraged to further attempt the potential application of surface photoalignment for modulating DLC columnar mesophases. There are mainly two types of orientations for DLC columnar mesophases, that is planar (edge-on) favoring for organic field-effect transistors (OFETs) and homeotropic (face-on) alignment preferred by light-emitting diodes (LEDs) or photovoltaic (PV) solar cells applications.[52,53]

As previously mentioned that the Pillar[5]-S10-Azo films showed long-term and high-temperature stability up to 150 °C covering the mesophase range of many low molar mass DLCs, together with their resistance to nonpolar solvents, such attributes made them possible to act as underlying directing films for regulating orientation of DLCs. The 2,3,6,7,10,11-hexakis(hexyloxy)triphenylene (TP6, **Figure 6**a) was a typical DLC compound[52,53] and well served as a contrast standard columnar mesophase of low molar mass for our investigation of triphenylene-based DLC polymers.[54] Herein, TP6 was employed as the columnar DLC to demonstrate the surface

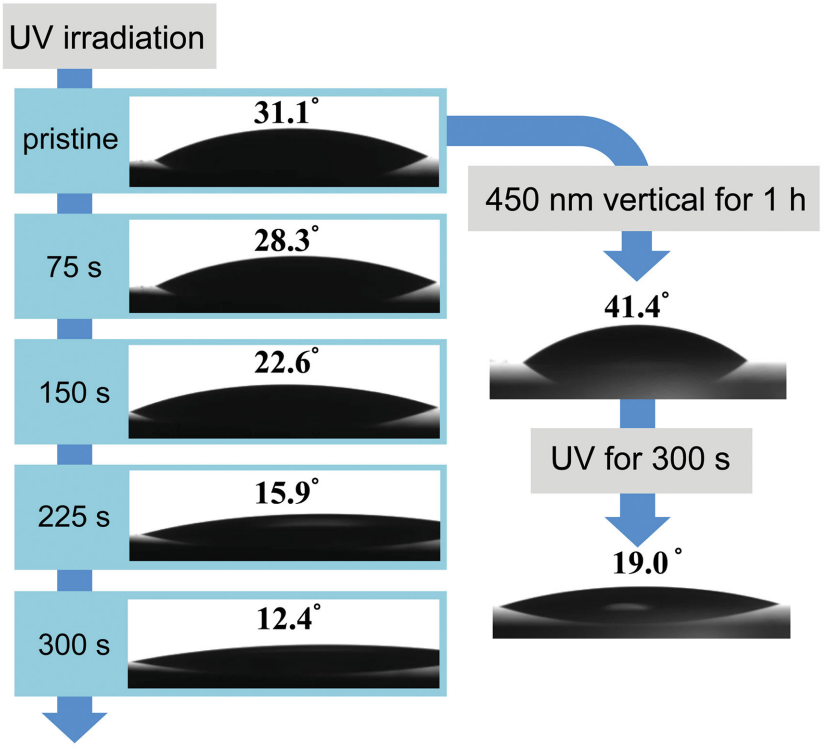

Figure 5. The contact angle evolution of an oil droplet on a Pillar[5]-S10-Azo thin film coated on quartz substrate, upon 365 nm UV irradiation for different times starting from the pristine film or after a long time (1 h) vertical exposure to nonpolarized actinic 450 nm visible light.

photoalignment mediated orientation of columnar mesophase, which exhibited a typical hexagonal columnar phase (Col_h) at the temperature range from 69 to 100 °C agreeing well with those reported by Boden et al.[55]

Pillar[5]-S10-Azo thin films of ≈100 nm thickness were prepared by spinning coating 5.0 wt% solution in THF onto quartz plates. The film was first vertically exposed to nonpolarized 450 nm light for 1 h and then irradiated by the same actinic light at an oblique incident angle of 45° for another 1.5 h through a photomask, which was essentially the same process as illustrated in Figure 3a only with a thinner film adopted here as the underneath directing layer. Then, 20 wt% solution of TP6 in *n*-hexane was spin-coated onto the quartz plates with precoated Pillar[5]-S10-Azo thin film to obtain the upper layer DLC films of ≈800 nm thickness (Figure 6a). The quartz-supported complex film system was studied and visualized under POM by slow heating at 1–2 °C min^{-1} on the sample chamber and photographed at selected temperatures. To well depict and differentiate two different layers in the multilayered complex film, in the following discussion "vertical" or "oblique" is employed to describe the alignment in Pillar[5]-S10-Azo film, while "homeotropic," "planar," and "random" are used for characterizing the orientation of the upper TP6 stacking columns of DLC columnar mesophase. First, as shown in Figure 6b–d we always kept the stripe direction in parallel with one of the crossed polarizers so that the POM images only reflected the birefringence changes of the upper layer TP discotic LC in view of under such conditions the underlying film exhibited a totally dark field regardless of the orientation of azobenzene chromophores (referring to Figure 3c). The pristine spin-coated DLC film at room temperature displayed dark field suggesting disordered TP6 arrangement in the as-prepared film (Figure 6b,e). When heated to the LC phase range, bright birefringent textures appeared in both stripe areas exposed to vertical or oblique actinic light and did not alter significantly with rotating the sample stage relative to the polarizer direction, indicating random or randomly planar orientation of TP6 columns.[28,56–58] Upon heating to 88 °C, the POM texture in stripes where Pillar[5]-S10-Azo film was obliquely aligned was much denser than that in vertically aligned ones (Figure 6c,f). Further heating to 94 °C near the clearing point and annealing, the stripe patterns presented remarkable contrast (Figure 6d), wherein the POM texture in obliquely aligned stripes faded away into dark field manifesting homeotropic orientation of TP6 columns,[28] while the birefringent texture in vertically aligned stripes changed little, indicating still random arrangement of TP6 columns (Figure 6g). On the other hand, homeotropic orientation of TP6 columns of DLC columnar mesophase on both vertically and obliquely aligned stripes was obtained when slowly cooling down at 0.5 °C min^{-1} from isotropic melts, as implied by the dark POM field under crossed polarizers and dendritic patterns of Col_h phase observed under parallel polarizers (Figure S30, Supporting Information).[57,59] The experimental results suggested that homeotropic orientation of the TP6 columns was formed predominantly irrespective of the underlying surface alignment upon slowly cooling from their isotropic state, while upon heating, obliquely aligned film surface of Pillar[5]-S10-Azo induced a significantly promoted homeotropic orientation for discotic TP6 columns than vertically aligned surface did. Moreover, upon fast cooling at about 20 °C min^{-1} from the isotropic state to room temperature, obvious macroscopic migration of TP6 molecules onto obliquely aligned stripes was clearly observed, leaving sporadically dispersed TP6 dewetting droplets on the vertically aligned stripes manifesting significant depletion region (Figure S31, Supporting Information). Such migration might also partially account for the aforementioned denser texture at 88 °C in obliquely aligned stripes based on the preferred wetting of TP6 discotic molecules on obliquely aligned areas than on vertically aligned surface. The main driving factor for the migration that leads to denser POM texture in obliquely aligned stripes is supposed to be the surface tension gradient due to free energy difference of underlying different directionally photoaligned azobenzene layer.

Although the detailed mechanism of the prevailingly induced homeotropic orientation on the obliquely photoaligned Pillar[5]-S10-Azo film surface was not clearly

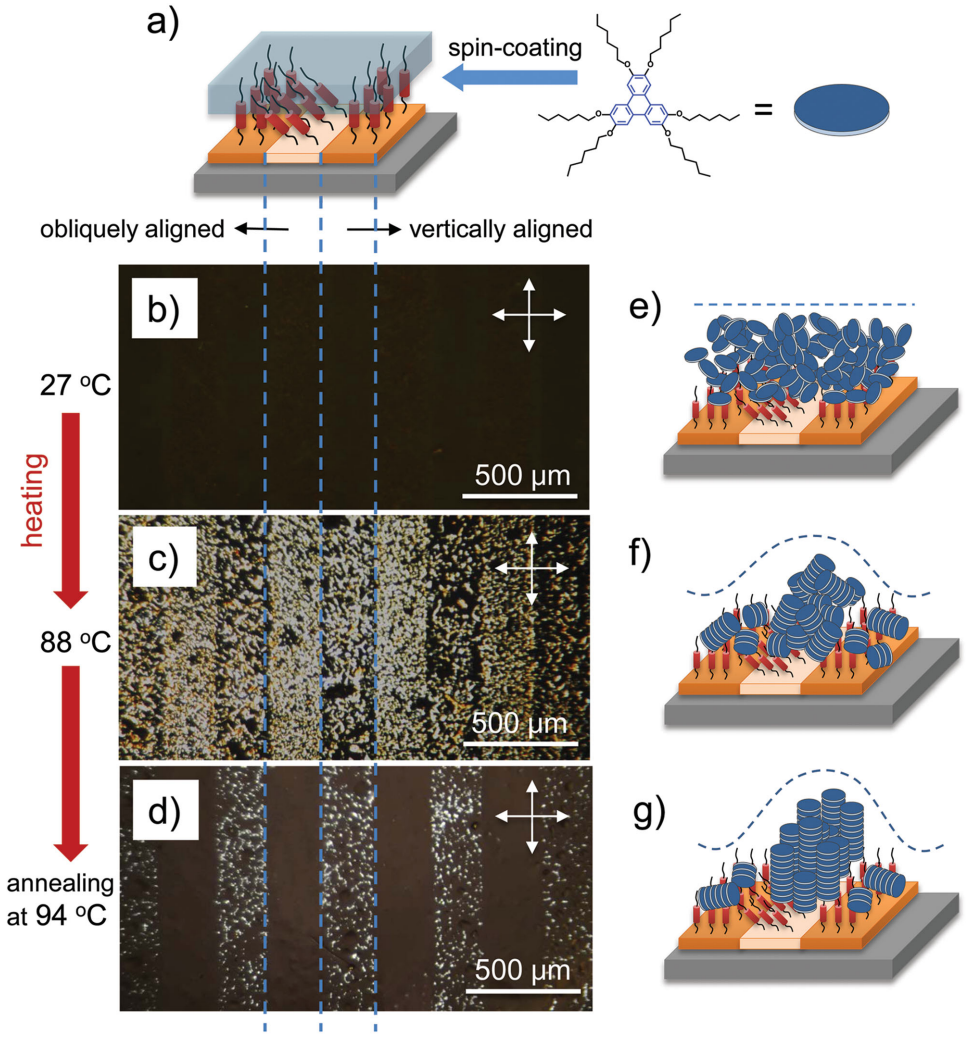

Figure 6. Photoaligned surface-mediated migration and orientation of DLC columnar mesophases on pillararene-based macrocyclic azobenzene mesomorphic thin films. a) Schematically showing the multilayered complex film with stripe-patterned vertically or obliquely aligned azobenzene chromophores and the molecular structure of TP6 discogen. b–d) Evolution of POM micrographs of the complex film with upper layer of a TP6 columnar LC film of ≈800 nm thickness and the underlying photoaligned Pillar[5]-S10-Azo film of ≈100 nm thickness, from 27 °C, upon heating to 88 °C, then annealing at 94 °C. The white crossed arrows indicate the POM crossed polarizers. e–g) Schematic illustration of the proposed packing structure, alignment, and distribution evolution of the upper layer TP6-based DLC on the underlying photoaligned stripe-patterned Pillar[5]-S10-Azo thin film corresponding to POM images in (b–d), respectively.

understood at present, the enhanced wettability of TP6 on such a surface obviously accelerated the homeotropic orientation of TP6 columns, which was reminiscent of the report that chemical treatments of indium tin oxide (ITO) substrate were shown to be efficient to prevent DLC thin film from dewetting and thus promising with better performance for optoelectronic applications.[60,61] Despite herein the preliminary study of the photoaligned Pillar[5]-S10-Azo film did not show sufficient amplifying effect to act as a "command surface," the vertically or obliquely aligned film surface really demonstrated evidently different wettability and even capability of modulating TP6-based DLC columnar mesophase orientation, which might provide a new approach and serve as photoresponsive directing layer for achieving orientation of DLCs in thin film devices.

3. Conclusions

Pillararene-based macrocyclic azobenzene liquid crystalline PRMs have been well prepared for the first time. The tubular pillar[5]arene-based macrocyclic framework provides sufficient free volume for azobenzene moieties to achieve reversible photoisomerization and light-induced alignment. Both Pillar[5]-S10-Azo and Pillar[5]-S4-Azo with variant length spacers showed wide temperature range lamellar LC mesophases and excellent film-formation property. Pillar[5]-S10-Azo films of longer spacers displayed better photoresponse performance as demonstrated by light-triggered modulation of surface free energy, wettability, and even photoaligned surface-mediated orientation of TP6-based DLC columnar mesophases. In view of their readily achievement of alignment via simple actinic light

irradiation of selected wavelengths or just changing incident directions, pillararene-based macrocyclic azobenzenes represent novel promising well-defined LC PRMs for film surface modulation and fascinating photoalignment directing agents.

4. Experimental Section

Materials: All reagents were commercially available and most of them were used without further purification, except that some solvents were dried by standard methods. The DLC used in this article, namely 2,3,6,7,10,11-hexakis(hexyloxy)triphenylene (note as TP6), was synthesized according to the literature in our laboratory.[54]

Instrumentation: NMR spectra were recorded on a Bruker DPX 300 spectrometer or a Bruker Avance III 400 spectrometer with TMS as the internal standard. Electrospray ionization mass spectra (ESI-MS) were acquired on a Finnigan Mat TSQ 7000 instrument. High-resolution electrospray ionization mass spectra (HR-ESI-MS) were recorded on an Agilent 6540Q-TOF LCMS equipped with an electrospray ionization (ESI) probe operating in positive-ion mode with direct infusion. The melting points were collected on an X-4 digital melting point apparatus without correction. Elemental analyses (EA) were carried out with an Elementar Vario Micro. MALDI-TOF mass spectrometry were carried out on an Autoflex mass spectrometer (Bruker Daltonics) operating in reflected mode. HPLC experiments were performed on a Shimadzu HPLC (type: UFLC) equipped with PDA as the detector and LC Solution as the control system, by using a Thermo Syncronis C18 reverse-phase column (4.6 mm × 250 mm, particle size: 5 μm). The DSC thermograms were recorded on a Perkin-Elmer Pyris I calorimeter equipped with a cooling accessory and under a nitrogen atmosphere upon heating or cooling at a rate of 10 °C min^{-1}. The phase transitions and LC textures were also investigated and photographed employing POM with equipment associated with a Leitz-350 heating stage and an Nikon (D3100) digital camera. X-ray scattering experiments were performed with a high-flux small-angle X-ray scattering instrument (SAXSess mc^2, Anton Paar) equipped with Kratky block-collimation system and a temperature control unit. Both SAXS and WAXS were simultaneously recorded on an imaging plate (IP) that extended to high-angle range (the q range covered by the IP was from 0.06 to 29 nm^{-1}, $q = 4\pi\sin\theta/\lambda$, where the wavelength λ is 0.1542 nm of Cu Kα radiation and 2θ is the scattering angle) at 40 kV and 50 mA. Typically, the powder sample was encapsulated with aluminum foil during the measurement and the obtained X-ray analysis data were processed with the associated SAXSquant software 3.80 (supplied by Anton Paar GmbH).

Film Preparation and Photoalignment: The thin films of LC samples on various substrates were prepared through spin-coating using the CHINAPONY KW-8A spin coater; then all the prepared films were completely dried under vacuum at room temperature and the thickness of the films was measured via Veeco Dektak 150 profilometer. Light irradiation was performed using Hg–Xe lamp (CHF-XM500W power system, China) through a band-pass filter (365 or 450 nm). Contact angle measurement was performed with a KSV CAM200 optical contact angle analyzer. In most cases, films of Pillar[5]-S10-Azo or Pillar[5]-S4-Azo with average thickness of 350 nm on quartz plates were prepared by spin-coating 10 wt% THF solution of corresponding LC samples. Specially, to avoid disturbance from the birefringence of Pillar[5]-S10-Azo layer in the multilayer complex film for photoaligned surface-mediated DLC orientation investigation, relatively thinner films of ≈100 nm thickness on quartz plates were employed, and they were obtained by spin-coating 5 wt% THF solution of Pillar[5]-S10-Azo. As the upper layer, relatively thicker films of TP6 were prepared by spin-coating 20 wt% *n*-hexane solution, then the thicknesses were measured to be ≈800 nm after subtraction of the underlying Pillar[5]-S10-Azo layer.

Synthesis and Characterization: Synthesis and relevant characterization details are provided in the Supporting Information.

Supporting Information

Supporting Information is available from the Wiley Online Library or from the author.

Acknowledgements

S.P. and M.F.N. contributed equally to this work. This work was supported by the National Natural Science Foundation of China (Grants 20874044 and 91227106) and also partially by Program for Changjiang Scholars and Innovative Research Team in University and the National Science Fund for Talent Training in Basic Science (No. J1103310). We would like to thank Dr. Shu Sun for her synthetic work at the early stage. S.P. thanks Mr. Xin Chen for his kind help with thin film preparation and characterization.

Received: March 9, 2015
Revised: April 10, 2015
Published online: May 7, 2015

[1] K. Ichimura, S. Oh, M. Nakagawa, *Science* **2000**, *288*, 1624.
[2] J. Berna, D. A. Leigh, M. Lubomska, S. M. Mendoza, E. M. Pérez, P. Rudolf, G. Teobaldi, F. Zerbetto, *Nat. Mater.* **2005**, *4*, 704.
[3] F. Ercole, T. P. Davis, R. A. Evans, *Polym. Chem.* **2010**, *1*, 37.
[4] F. Xia, L. Jiang, *Adv. Mater.* **2008**, *20*, 2842.
[5] M. Banghart, K. Borges, E. Isacoff, D. Trauner, R. H. Kramer, *Nat. Neurosci.* **2004**, *7*, 1381.
[6] J. E. Stumpel, D. J. Broer, A. P. Schenning, *Chem. Commun.* **2014**, *50*, 15839.
[7] K. Ichimura, *Chem. Rev.* **2000**, *100*, 1847.
[8] A. Natansohn, P. Rochon, *Chem. Rev.* **2002**, *102*, 4139.
[9] T. Ikeda, *J. Mater. Chem.* **2003**, *13*, 2037.
[10] M. O'Neill, S. M. Kelly, *J. Phys. D: Appl. Phys.* **2000**, *33*, R67.
[11] G. S. Kumar, D. C. Neckers, *Chem. Rev.* **1989**, *89*, 1915.
[12] C. J. Barrett, J. Mamiya, K. G. Yager, T. Ikeda, *Soft Matter* **2007**, *3*, 1249.
[13] H. Yu, *J. Mater. Chem. C* **2014**, *2*, 3047.
[14] H. Yu, T. Iyoda, T. Ikeda, *J. Am. Chem. Soc.* **2006**, *128*, 11010.
[15] H. Yu, S. Asaoka, A. Shishido, T. Iyoda, T. Ikeda, *Small* **2007**, *3*, 768.
[16] S. Furumi, M. Kidowaki, M. Ogawa, Y. Nishiura, K. Ichimura, *J. Phys. Chem. B* **2005**, *109*, 9245.
[17] T. Ubukata, M. Hara, K. Ichimura, T. Seki, *Adv. Mater.* **2004**, *16*, 220.
[18] Y. Morikawa, S. Nagano, K. Watanabe, K. Kamata, T. Iyoda, T. Seki, *Adv. Mater.* **2006**, *18*, 883.
[19] A. Ambrosio, L. Marrucci, F. Borbone, A. Roviello, P. Maddalena, *Nat. Commun.* **2012**, *3*, 989.
[20] J. W. Weener, E. W. Meijer, *Adv. Mater.* **2000**, *12*, 741.
[21] E. Blasco, J. L. Serrano, M. Piñol, L. Oriol, *Macromolecules* **2013**, *46*, 5951.
[22] K. Ichimura, Y. Suzuki, T. Seki, A. Hosoki, K. Aoki, *Langmuir* **1988**, *4*, 1214.
[23] T. Seki, M. Sakuragi, Y. Kawanishi, T. Tamaki, R. Fukuda, K. Ichimura, Y. Suzuki, *Langmuir* **1993**, *9*, 211.
[24] K. Aoki, T. Seki, Y. Suzuki, T. Tamaki, A. Hosoki, K. Ichimura, *Langmuir* **1992**, *8*, 1007.
[25] K. Ichimura, *J. Photochem. Photobiol. A* **2003**, *158*, 205.
[26] K. Ichimura, S. Furumi, S. Morino, M. Kidowaki, M. Nakagawa, M. Ogawa, Y. Nishiura, *Adv. Mater.* **2000**, *12*, 950.
[27] S. Furumi, K. Ichimura, *J. Phys. Chem. B* **2007**, *111*, 1277.
[28] Z. H. Al-Lawati, R. J. Bushby, S. D. Evans, *J. Phys. Chem. C* **2013**, *117*, 7533.
[29] M. Xue, Y. Yang, X. Chi, Z. Zhang, F. Huang, *Acc. Chem. Res.* **2012**, *45*, 1294.

[30] P. J. Cragg, K. Sharma, *Chem. Soc. Rev.* **2012**, *41*, 597.
[31] T. Ogoshi, T. Yamagishi, *Eur. J. Org. Chem.* **2013**, *2013*, 2961.
[32] H. Zhang, Y. Zhao, *Chem. Eur. J.* **2013**, *19*, 16862.
[33] T. Ogoshi, T. Yamagishi, *Chem. Commun.* **2014**, *50*, 4776.
[34] Q. Duan, Y. Cao, Y. Li, X. Hu, T. Xiao, C. Lin, Y. Pan, L. Wang, *J. Am. Chem. Soc.* **2013**, *135*, 10542.
[35] Y. Cao, X. Hu, Y. Li, X. Zou, S. Xiong, C. Lin, Y. Shen, L. Wang, *J. Am. Chem. Soc.* **2014**, *136*, 10762.
[36] H. Zhang, N. L. Strutt, R. S. Stoll, H. Li, Z. Zhu, J. F. Stoddart, *Chem. Commun.* **2011**, *47*, 11420.
[37] G. Yu, C. Han, Z. Zhang, J. Chen, X. Yan, B. Zheng, S. Liu, F. Huang, *J. Am. Chem. Soc.* **2012**, *134*, 8711.
[38] T. Ogoshi, K. Yoshikoshi, T. Aoki, T. Yamagishi, *Chem. Commun.* **2013**, *49*, 8785.
[39] T. Ogoshi, K. Kida, T. Yamagishi, *J. Am. Chem. Soc.* **2012**, *134*, 20146.
[40] I. Nierengarten, S. Guerra, M. Holler, J. Nierengarten, R. Deschenaux, *Chem. Commun.* **2012**, *48*, 8072.
[41] I. Nierengarten, S. Guerra, M. Holler, L. Karmazin-Brelot, J. Barbera, R. Deschenaux, J. Nierengarten, *Eur. J. Org. Chem.* **2013**, *2013*, 3675.
[42] R. Rathore, J. K. Kochi, *J. Org. Chem.* **1995**, *60*, 7479.
[43] T. Ogoshi, S. Kanai, S. Fujinami, T. Yamagishi, Y. Nakamoto, *J. Am. Chem. Soc.* **2008**, *130*, 5022.
[44] D. Cao, Y. Kou, J. Liang, Z. Chen, L. Wang, H. Meier, *Angew. Chem. Int. Ed.* **2009**, *48*, 9721.
[45] N. L. Strutt, H. Zhang, S. T. Schneebeli, J. F. Stoddart, *Acc. Chem. Res.* **2014**, *47*, 2631.
[46] a) T. Ogoshi, R. Shiga, M. Hashizume, T. Yamagishi, *Chem. Commun.* **2011**, *47*, 6927; b) I. Nierengarten, M. Nothisen, D. Sigwalt, T. Biellmann, M. Holler, J.-S. Remy, J.-F. Nierengarten, *Chem. Eur. J.* **2013**, *19*, 17552; c) H. M. Deng, X. Y. Shu, X. S. Hua, J. Li, X. S. Jia, C. J. Li, *Tetrahedron Lett.* **2012**, *53*, 4609.
[47] S. Zimmermann, J. H. Wendorff, C. Weder, *Chem. Mater.* **2002**, *14*, 2218.
[48] N. Hosono, T. Kajitani, T. Fukushima, K. Ito, S. Sasaki, M. Takata, T. Aida, *Science* **2010**, *330*, 808.
[49] A. Bobrovsky, N. Boiko, V. Shibaev, J. Stumpe, *J. Photochem. Photobiol. A* **2004**, *163*, 347.
[50] M. Moritsugu, T. Ishikawa, T. Kawata, T. Ogata, Y. Kuwahara, S. Kurihara, *Macromol. Rapid Commun.* **2011**, *32*, 1546.
[51] Y. Kuwahara, M. Kaji, J. Okada, S. Kim, T. Ogata, S. Kurihara, *Mater. Lett.* **2013**, *113*, 202.
[52] S. Kumar, *Chemistry of Discotic Liquid Crystals: From Monomers to Polymers*, CRC Press, Boca Raton, FL **2010**.
[53] R. J. Bushby, S. M. Kelly, M. O'Neill, *Liquid Crystalline Semiconductors: Materials, Properties and Applications*, Springer, Dordrecht, The Netherlands **2013**.
[54] a) B. Wu, B. Mu, S. Wang, J. F. Duan, J. L. Fang, R. S. Cheng, D. Z. Chen, *Macromolecules* **2013**, *46*, 2916; b) B. Mu, B. Wu, S. Pan, J. L. Fang, D. Z. Chen, *Macromolecules* **2015**, *48*, 2388.
[55] N. Boden, R. J. Bushby, J. Clements, *J. Chem. Phys.* **1993**, *98*, 5920.
[56] Z. H. Al-Lawati, B. Alkhairalla, J. P. Bramble, J. R. Henderson, R. J. Bushby, S. D. Evans, *J. Phys. Chem. C* **2012**, *116*, 12627.
[57] J. Wang, Z. He, Y. Zhang, H. Zhao, C. Zhang, X. Kong, L. Mu, C. Liang, *Thin Solid Films* **2010**, *518*, 1973.
[58] N. Terasawa, H. Monobe, K. Kiyohara, Y. Shimizu, *Chem. Commun.* **2003**, 1678.
[59] T. Osawa, T. Kajitani, D. Hashizume, H. Ohsumi, S. Sasaki, M. Takata, Y. Koizumi, A. Saeki, S. Seki, T. Fukushima, T. Aida, *Angew. Chem. Int. Ed.* **2012**, *124*, 8114.
[60] S. Archambeau, I. Seguy, P. Jolinat, J. Farenc, P. Destruel, T. P. Nguyen, H. Bock, E. Grelet, *Appl. Surf. Sci.* **2006**, *253*, 2078.
[61] B. R. Kaafarani, *Chem. Mater.* **2011**, *23*, 378.